


Enabling a Ductile Failure of Laminated Glass Beams with Iron-Based Shape Memory Alloy (Fe-SMA) Strips

Conference Paper**Author(s):**

[Silvestru, Vlad-Alexandru](#) ; Deng, Zhikang; Michels, Julien; Taras, Andreas

Publication date:

2022-09

Permanent link:

<https://doi.org/10.3929/ethz-b-000580801>

Rights / license:

[Creative Commons Attribution 4.0 International](#)

Originally published in:

ce/papers 5(4), <https://doi.org/10.1002/cepa.1839>

ORIGINAL ARTICLE

SDSS 2022
The International Colloquium on Stability
and Ductility of Steel Structures
14-16 September, University of Aveiro, PortugalErnst & Sohn
A Wiley Brand

Enabling a Ductile Failure of Laminated Glass Beams with Iron-Based Shape Memory Alloy (Fe-SMA) Strips

Vlad-Alexandru Silvestru¹, Zhikang Deng¹, Julien Michels², Andreas Taras¹

Correspondence

Dr. Vlad-Alexandru Silvestru
ETH Zurich
Institute of Structural Engineering
Stefano-Franscini-Platz 5
8093 Zurich, Switzerland
Email: silvestru@ibk.baug.ethz.ch

Abstract

Laminated glass beams are used as structural elements to support transparent roofs or to transfer wind loads acting on transparent facades. However, in case of breakage, laminated glass beams only exhibit a low residual load-carrying capacity provided by the interlayers. A more efficient solution is to add a filigree ductile reinforcement on the tension side of the laminated glass beams, for instance by adhesive bonding. By these means, the post-cracking behaviour of the beams and their redundancy can be improved and a ductile failure behaviour can be achieved. Moreover, an additional pre-stressing of this reinforcement allows increasing the initial glass cracking resistance. Despite their obvious potential, an application of pre-stressed laminated glass beams in real projects is prevented by the rather complicated necessary procedures for pre-stressing. This contribution discusses first experimental results on a novel concept for pre-stressed laminated glass beams with adhesively bonded strips made of an iron-based shape memory alloy (Fe-SMA). The pre-stress can be applied in this case by heating up the Fe-SMA. The feasibility of the concept is analysed based on results from four-point-bending tests on medium-scale simple, reinforced and pre-stressed laminated glass beams.

Keywords

Iron-based shape memory alloy, Reinforced laminated glass beam, Post-tensioned laminated glass beam, Ductile failure, Residual load-carrying capacity, Four-point-bending test

1 Introduction

The structural use of the material glass has increased significantly in the last decades, especially in the area of the building envelope in the form of laminated glass beams or as large laminated glass panels. Laminated glass beams are mostly used as structural elements to support transparent roofs, to transfer wind loads acting on transparent facades (see example in Figure 1), or for smaller interior structures like glass staircases and glass bridges. Glass, however, is a brittle material and in case of breakage, laminated glass beams exhibit therefore only a low residual load-carrying capacity due to the structural capacity of the interlayers. A common approach for today's structural design of laminated glass beam applications is to oversize the beams, for example by assuming that the laminated glass beams have to be able to support the occurring loads even if one of the exterior glass layers is broken. This results in larger cross-sections and inefficient use of material.

A more efficient approach for improving the structural performance and especially the residual load-carrying capacity of laminated glass beams is adding a filigree ductile reinforcement on their tension side, for instance

by adhesive bonding. This allows to improve the post-cracking behaviour of the beams and to achieve a ductile failure behaviour. With a suitable choice of materials and proper sizing, such reinforced laminated glass beams can carry after breakage of all glass layers even loads higher than the load leading to initial glass crack. The reinforcement can be applied either along one of the edges (e.g. a glass beam supporting a roof, where tension is always occurring at the bottom edge) or along both of the edges (e.g. a glass fin in a façade, where tension can occur at both edges due to wind suction and wind pressure).

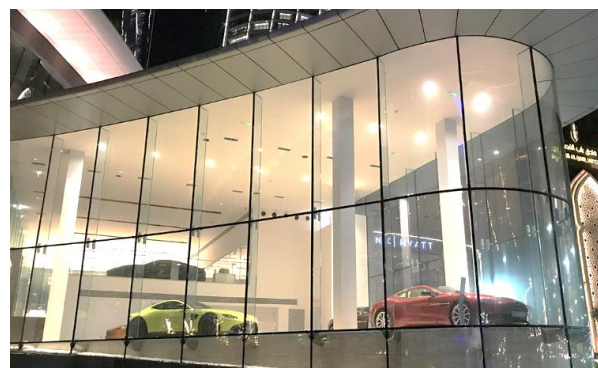


Figure 1 Example of laminated glass beams used as supporting structural elements for a transparent façade. Source: V.A. Silvestru/ETH Zurich

1. ETH Zurich, Institute of Structural Engineering, Zurich, Switzerland.
2. re-fer AG, Seewen, Switzerland.

This is an open access article under the terms of the Creative Commons Attribution License, which permits use, distribution and reproduction in any medium, provided the original work is properly cited.

Open access funding provided by Eidgenössische Technische Hochschule Zurich.

WOA Institution: Eidgenössische Technische Hochschule Zurich

Consortia Name: CSAL

© 2022 The Authors. Published by Ernst & Sohn GmbH. · ce/papers 5 (2022), No. 4

<https://doi.org/10.1002/cepa.1839>

wileyonlinelibrary.com/journal/cepa

948

The initial glass cracking resistance of the reinforced laminated glass beams can be increased even further by an additional pre-stressing of the reinforcement tendons. Reinforced and pre-stressed (post-tensioned) glass beams have been investigated before in different research projects (see overview in [1]). For most of these investigations, rods or strips made of steel, stainless steel or fibre-reinforced plastics were used. A differentiation can be made between laminated glass beams with tendons positioned laterally outside the glass beams (see for example [2]-[4]) and beams with tendons positioned at the edge of the glass beams (see for example [2], [5]-[8]). However, for all previously investigated mechanically pre-stressed laminated glass beams rather complex setups and procedures, often including hydraulic jacks, were necessary.

This contribution introduces a novel concept for manufacturing pre-stressed laminated glass beams by using adhesively bonded iron-based shape memory alloy (Fe-SMA) strips as tendons. This shape memory alloy (SMA) was developed for applications in the construction field and, similar to other SMAs, has the property of remembering its initial shape after two phase transformations. The first phase transformation from austenite to martensite is triggered by deforming or pre-straining, while the second one from martensite back to austenite (activation) is triggered by heating the material. More material-related details on the Fe-SMA are provided in section 2.2.

The necessary production steps for the novel concept are illustrated in Figure 2 for a laminated glass beam with bonded tendons along both edges. The steps (i)-(iii) are carried out in the production facility for the Fe-SMA and result in coils of pre-strained Fe-SMA material.

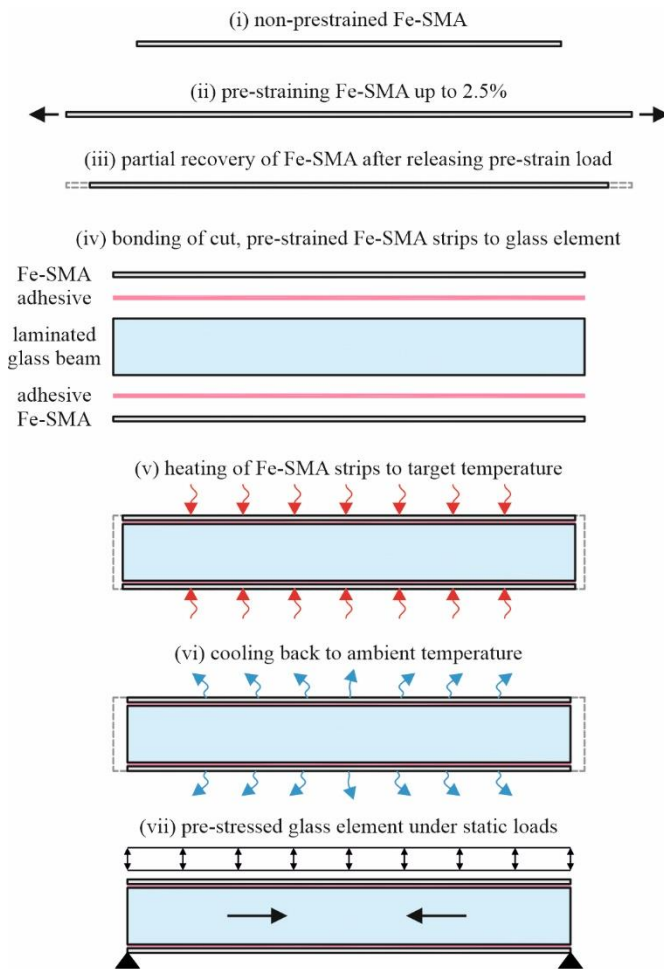


Figure 2 Schematic illustration of the production steps for pre-stressing laminated glass beams with Fe-SMA strips. Source: V.A. Silvestru/ETH Zurich

From the coils, strips of Fe-SMA can be cut to the necessary length and width and delivered to the building site or to a subsequent producer. In case of the pre-stressed glass beams, this subsequent producer would be a façade contractor. For the concept presented in this paper, the pre-strained Fe-SMA strips are then adhesively bonded to the edges of the laminated glass beams (iv). By heating the Fe-SMA strips to a target temperature (v), the second phase transformation is triggered and a certain fraction of the previously induced martensite transforms back to austenite. This translates into an effort of the strips to go back to their initial length before pre-straining and, since the strips are anchored by adhesive bonding, into a compressive pre-stress in the laminated glass. While cooling down back to ambient temperature (vi), the pre-stress level is further increased. After these production steps are completed, the pre-stressed laminated glass beams can be delivered to site, installed and subjected to static loads according to their planned use (vii).

The proposed concept is considered to allow a more easy-to-apply and, therefore, more efficient alternative for pre-stressed (post-tensioned) laminated glass beams. This paper discusses results from experimental investigations performed on medium-scale laminated, reinforced and pre-stressed glass beams, which were carried out to prove the feasibility of the novel concept.

2 Materials

2.1 Laminated glass beams

Laminated glass is a layered assembly consisting of two or more glass layers bonded together with interlayers made of plastic materials. For the laminated glass beams investigated in this paper, annealed soda-lime silicate glass without any thermal or chemical tempering and interlayers made of the ionoplast SentryGlas® were used. A cross section through one of the beams and the thicknesses of the different layers of the laminated glass beams are shown in Figure 3. Annealed soda-lime silica glass has a Young's modulus of 70'000 MPa, a characteristic bending strength of 45 MPa, a thermal shock resistance of 40 K and a thermal expansion coefficient of $9 \times 10^{-6} \text{ K}^{-1}$ according to EN 572-1 [9]. The properties of the interlayer material are strongly dependent on temperature and load duration. For the conditions of the performed four-point-bending tests (temperature of around 18 °C and loading speed of 1 mm/min), a Young's modulus of around 493 MPa can be assumed based on [10].

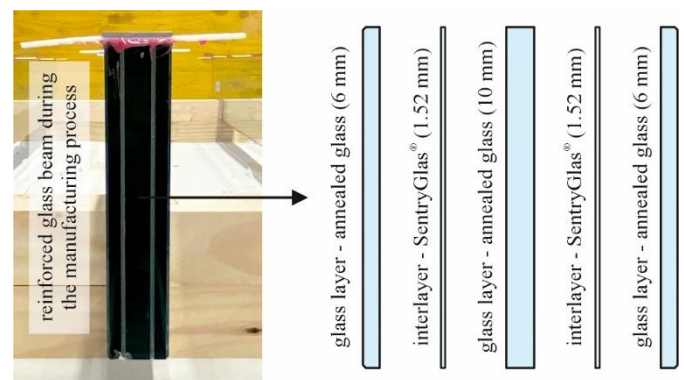


Figure 3 Illustration of the assembly of a laminated glass as used for the glass beams investigated in this paper. Source: V.A. Silvestru/ETH Zurich

2.2 Iron-based shape memory alloy tendons

The iron-based shape memory alloy (Fe-SMA) memory®-steel used for the reinforced and pre-stressed laminated glass beams investigated in

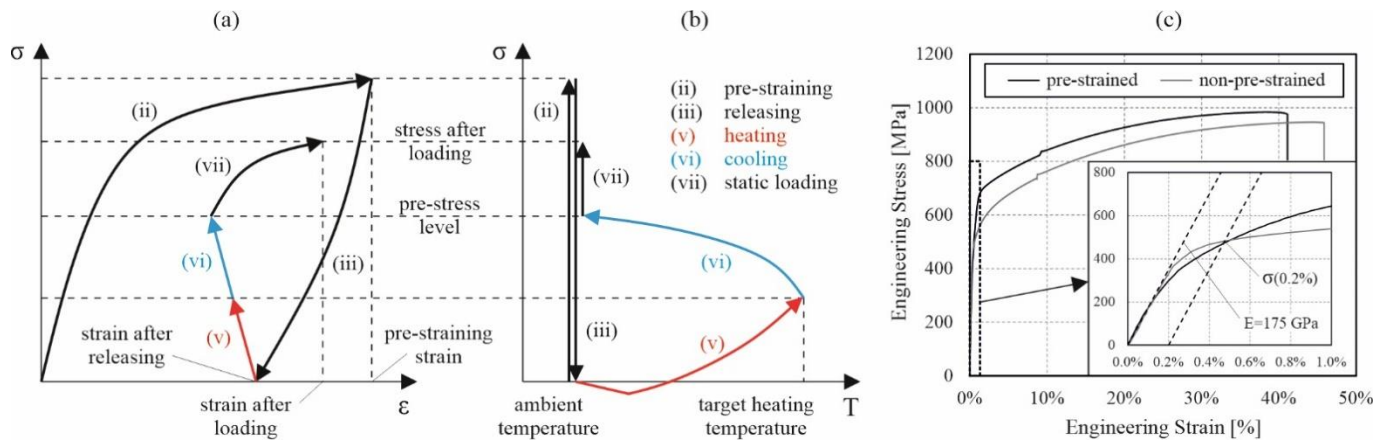


Figure 4 Qualitative stress vs. strain (a) and stress vs. temperature (b) behaviours of the Fe-SMA strips during pre-straining, activation and static loading and engineering stress vs. engineering strain curves for non-pre-strained and pre-strained Fe-SMA (c). Source: V.A. Silvestru/ETH Zurich

this contribution was developed by re-fer AG especially for the construction sector with the objective of creating permanent pre-stress forces in structural elements. The main applications of this material are reinforcing of existing concrete and steel structures. The Fe-SMA strips are currently produced as coils of sheet material with a width of 120 mm and a thickness of 1.5 mm. During the proposed production of pre-stressed laminated glass beams (see Figure 2), the Fe-SMA strips are subjected to several steps in which their stress level is modified. For explaining this stress development, Figure 4a-b show the interrelated qualitative stress vs. strain and stress vs. temperature relationships in the Fe-SMA during pre-straining, activation and static loading, adapted from [11] and [12].

The iron-based shape memory alloy can be applied in both phases (non-pre-strained or activated in the austenite phase and pre-strained in the martensite phase). As shown in [13] and in Table 1 as well as illustrated by the stress vs. strain curves plotted in Figure 4c, the mechanical material properties of the Fe-SMA slightly differ in the two phases. This has to be considered when analysing the results from the experiments as well as in future simulations or structural design calculations.

Table 1 Selected relevant mechanical material properties of the non-pre-strained and the pre-strained Fe-SMA (rounded values from [13])

Property	Non-pre-strained Fe-SMA	Pre-strained Fe-SMA
0.2% yield strength	480 MPa	490 MPa
Ultimate tensile strength	940 MPa	995 MPa
Elongation at failure	44%	41%

2.3 Mechanical properties of the used adhesive

For the reinforced and pre-stressed glass beams discussed in this paper, the two-component epoxy SikaPower®-1277 was used. This adhesive was previously used in research on shear connections between Fe-SMA strips and steel substrates (see [14]) as well as between Fe-SMA strips and glass substrates (see [13]), where it showed a promising performance. Selected relevant properties of the adhesive are provided in Table 2 based on [15]. The adhesive can be categorized as a high-strength, rather stiff adhesive, which does not allow for significant deformations before failure. Its glass transition temperature is also at a suitable level considered the maximum temperatures expected behind an insulated transparent façade.

Table 2 Selected relevant properties of the applied structural adhesive SikaPower®-1277 (values taken from the product data sheet [15])

Property	SikaPower®-1277
Colour	Light red
Open time / handling time (ISO 4587)	1 hour / 11 hours
Tensile strength (ISO 527)	30 MPa
Young's modulus (ISO 527)	2'000 MPa
Elongation at break (ISO 527)	4%
Tensile lap-shear strength (ISO 4587)	28 MPa
Glass transition temperature (ISO 6721)	67 °C

3 Methods

Three types of glass beams were experimentally investigated in four-point-bending: (i) laminated glass beams without any reinforcement (see Figure 5a), (ii) reinforced laminated glass beams (see Figure 5b) and (iii) pre-stressed laminated glass beams (see Figure 5c). For the reinforced and the pre-stressed ones, the Fe-SMA strips were adhesively bonded to the laminated glass beams in the laboratory of the Institute of Structural Engineering at ETH Zurich. Furthermore, the activation of the Fe-SMA strips in the case of the pre-stressed laminated glass beams was as well carried out in the same laboratory facilities. Fe-SMA strips were bonded along both glass beam edges, as it would make sense for glass fins in transparent façades. The dimensions as well as the type and position of the applied measurement instrumentation for the different beam types are illustrated in Figure 5.

3.1 Manufacturing of the reinforced glass beams

The manufacturing of the reinforced laminated glass beams consisted in adhesively bonding the Fe-SMA strips to the laminated glass beam edges. In a first step, the Fe-SMA strips were cleaned with acetone and sand-blasted to improve the adhesion to their surfaces. The bottom and top Fe-SMA strips were bonded to the vertically positioned laminated glass beams at an interval of two days. The bond areas were delimited with tapes and 10 mm wide Teflon spacers were positioned at pre-defined equal distances to ensure a relatively constant thickness of the adhesive joints of 1.5 mm. Before applying the adhesive, both the Fe-SMA and the glass edge surfaces were thoroughly cleaned with acetone for removing any remaining dust or grease. The adhesive was then

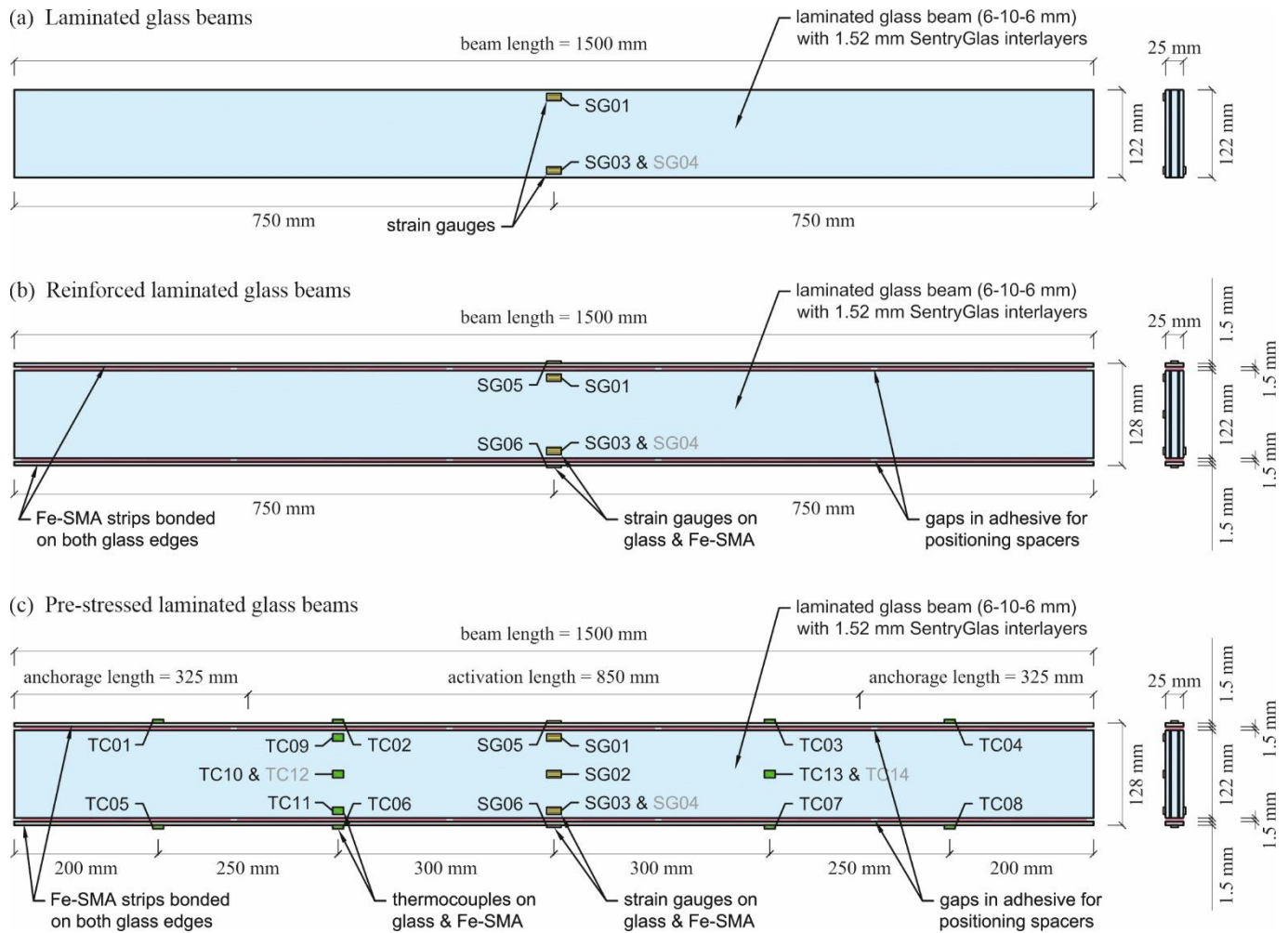


Figure 5 Specimen geometry and location of measurement instrumentation (strain gauges and thermocouples) for the laminated glass beams (a), the reinforced laminated glass beams (b) and the pre-stressed laminated glass beams (c). Source: V.A. Silvestru/ETH Zurich

applied from 195 ml dual cartridges with static mixers and hand application guns on both the Fe-SMA and the glass edge surfaces. Before pressing the two elements, with the Teflon spacers between them, against each other, the adhesive was tooled with a spatula. After removing the bond delimiting tapes, the specimens were left to cure over night with weights pressing on the Fe-SMA strips. All the steps were then repeated for the second Fe-SMA strips. Afterwards, the specimens were stored for two weeks in a climate chamber at 20 °C and 50% relative humidity before proceeding with application of measurement instrumentation, activation and testing. Three specimens were manufactured for each beam type as shown in Table 3.

Table 3 Specimen types and names

Specimen type	Specimen name
Laminated glass beams	BT-01-ref BT-02-ref BT-03-ref
Reinforced laminated glass beams	BT-04-SP-na BT-05-SP-na BT-06-SP-na (BT-06-SP-na had only one Fe-SMA strip adhesively bonded on the tension side)
Pre-stressed laminated glass beams	BT-10-SP-a BT-11-SP-a BT-12-SP-a

For the laminated glass beams, three strain gauges were applied in the middle of the beams, one near the top edge (compressed in the four-point-bending tests) on the front side of the beam and two near the

bottom edge (tensioned in the four-point-bending tests), one on the front and one on the back side of the beam. For the reinforced laminated glass beams, two additional strain gauges were applied on the Fe-SMA strips, one in the middle of the top strip and one in the middle of the bottom one. For the pre-stressed laminated glass beams, a further strain gauge was placed on the front side in the centre of the beams. The strain gauges on the glass surfaces were applied before the activation procedure, while those on the Fe-SMA strips only afterwards, not to damage them through the heating. In addition to strain gauges, a total of fourteen thermocouples of type K were applied on the Fe-SMA strip and on the glass surfaces to monitor the temperature development during the activation procedure.

3.2 Pre-stressing by electrical resistive heating

The phase transformation of the Fe-SMA from martensite back to austenite (activation) was triggered by electrical resistive heating. This method allows to target specific temperature values by applying an electric current to the Fe-SMA. The method was assessed before for strengthening metallic girders with Fe-SMA plates (see [16]) as well as in a preliminary study for activating Fe-SMA strips bonded to glass panels (see [13]). Details on the procedure can also be found in [12].

The setup for the activation procedure to transform reinforced into pre-stressed laminated glass beams is shown in Figure 6. The reinforced laminated glass beams were positioned on supports made of timber. Layers of Teflon were applied between the glass beams and the timber parts to allow a better sliding. For the applied current, a single circuit was used going through both the top and the bottom strip.

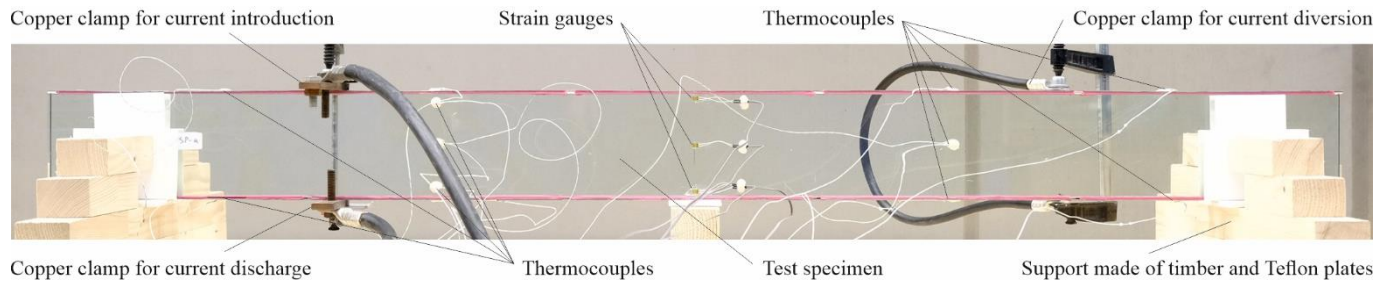


Figure 6 Setup used for pre-stressing of the reinforced glass beams by electrical resistive heating of the Fe-SMA strips. Source: V.A. Silvestru/ETH Zurich

The current was introduced in the top strip on the left side of the beam, was diverted from the top strip to the bottom one with a copper clamp on the right side of the beam and was discharged from the bottom strip on the right side of the beam (see Figure 6). The copper clamps were not fixed directly at the end of the beams, but at a distance of around 325 mm from the ends. This distance ensured long enough anchorage lengths in which the adhesive is not heated up and therefore not damaged during activation. An amperage of 200 A was applied with an electrical power supply unit provided by re-fer AG until a target temperature of 160 °C was measured with one of the thermocouples positioned on the Fe-SMA strips. The amperage and the target temperature were chosen based on the results from previous investigations (see [13] and [17]).

3.3 Four-point-bending tests

All nine beams were tested in four-point-bending with the objective to evaluate the benefit in initial glass crack resistance and residual load-carrying capacity achieved by the reinforced and especially by the pre-stressed laminated glass beams with adhesively bonded Fe-SMA strips compared to the beams without any reinforcement. The tests were performed on a Schenck servo-hydraulic testing machine allowing a maximum force of 1600 kN. The test setup with its main components can be seen in Figure 7a, while Figure 7b shows the distances between the supports as well as between the loads.

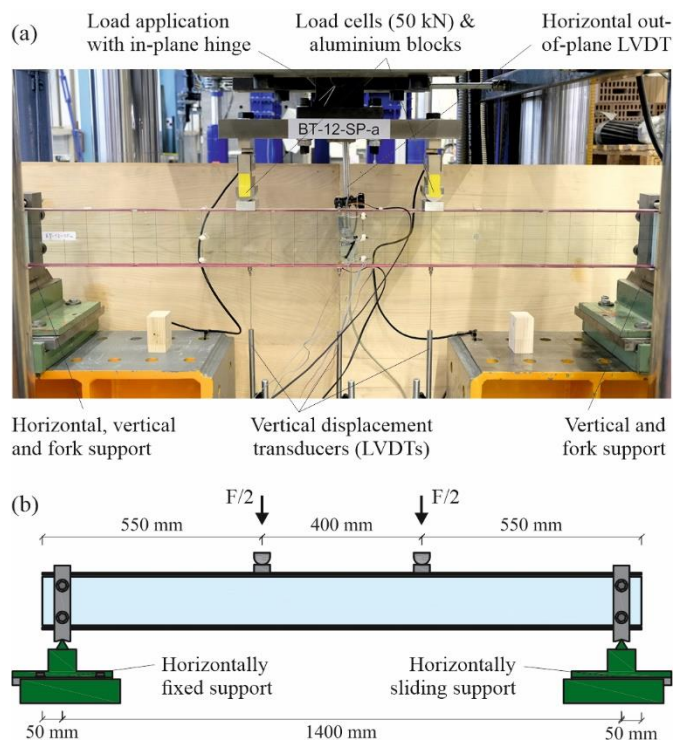


Figure 7 Main components of the test setup used for the four-point-bending tests (a) and main dimensions of the static system (b). Source: V.A. Silvestru/ETH Zurich

The load was applied displacement-controlled with a displacement rate of 1 mm/min until a displacement of 15 mm, 2 mm/min until 45 mm and 4 mm/min until failure. The load-distributing beam was hinge-connected to the machine allowing an in-plane rotation. Between the load-distributing beam and the glass beams, two load cells able to measure forces of up to 50 kN were positioned at the two load introduction points. The load introduction was realised with two half-cylindrical steel parts positioned at a distance of 400 mm to each other. Aluminium blocks were positioned between the half-cylindrical parts and the top edge of the beams for obtaining a larger contact area for force transfer. The beams were placed in two fork-shaped steel parts at a distance of 1400 mm. These steel parts were standing on existing support elements (green parts in Figure 7) with triangular steel rods at their top. As a result the glass beams were simply supported at their ends in vertical direction, allowing rotation in in-plane direction, but not allowing torsional rotations. The support on the left in Figure 7 was fixed, while that on the right allowed sliding thanks to Teflon layers. The dimensions both of the glass beam specimens and of the test setup were chosen in agreement with those used in [8] for allowing a comparison between results. Beside the machine displacement, three displacement transducers were used below the glass beams to measure the vertical in-plane deflections and an additional one was used behind the glass beams to measure an eventual horizontal out-of-plane displacement. The tests were performed at a room ambient temperature of around 18 °C.

4 Results and discussion

4.1 Pre-stressing results

During the activation of the Fe-SMA strips by electrical resistive heating, the temperature on the Fe-SMA and glass surfaces as well as strains on the glass surfaces were monitored over a time of two hours with thermocouples and strain gauges, respectively. The results of these measurements are shown for one representative test specimen (BT-12-SP-a) in the diagrams from Figure 8. From Figure 8a it can be observed that the temperatures measured outside the activation length TC (01;04;05;08) remain constant. This confirms that the current flows only in the desired area of the Fe-SMA strips and that the adhesive in the anchorage areas is not heated. Within the activation areas, the temperature in the top strip TC (02;03) reaches a slightly higher value than that in the bottom one TC (06;07). This is in agreement with the fact that the maximum strain measured in the glass near the top edge (SG01) is a little higher than that measured by the strain gauges near the bottom edge (SG03 and SG04). The temperature on the glass surfaces near the Fe-SMA strips TC (09;11) is only increased by around 20 °C, which is not problematic for thermal shocks. The temperatures in the middle of the glass beams TC (10;12;13;14) increase significantly less. Regarding strains, it can be observed from Figure 8b that in the beginning of the activation procedure higher strains are induced near the edges of the laminated glass beams compared to their centre. However, after all materials cool back to ambient room temperature, the strains measured with the four strain gauges on the glass surfaces reach relatively constant values of around 90-100 $\mu\text{m}/\text{m}$.

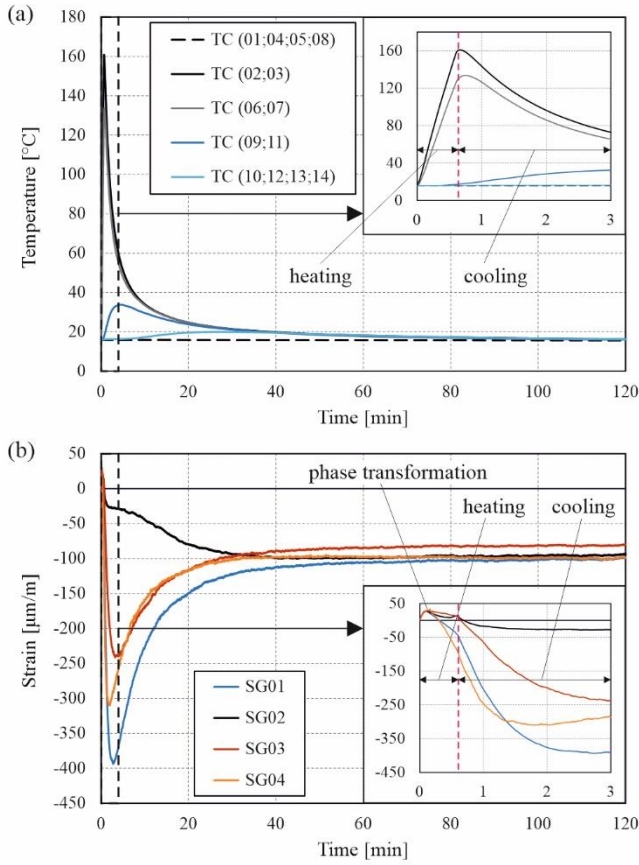


Figure 8 Temperature and strain development over time for one representative test specimen (BT-12-SP-a). Source: V.A. Silvestru/ETH Zurich

From the temperature and strain developments during the first minute of the activation process, it can be observed that tensile strains are measured on the glass surfaces until a temperature of around 45 °C is reached by the strips. This is the temperature at which the phase transformation is triggered.

Table 4 summarizes selected values determined based on the measurements conducted for all three pre-stressed laminated glass beams. From the differences of the maximum reached temperatures in the Fe-SMA and in the glass and the times after which these temperatures were reached, it can be concluded that the adhesives offer a relatively good thermal insulation. The strain in the glass after 120 minutes $\epsilon_{\text{glass},120\text{min}}$ is determined as an average of the values measured by the four strain gauges. With this value and the Young's modulus of glass $E_{\text{glass}} = 70'000 \text{ MPa}$, the stress in the glass $\sigma_{\text{glass},120\text{min}}$ can be roughly determined with Equation (1):

$$\sigma_{\text{glass},120\text{min}} = \epsilon_{\text{glass},120\text{min}} \cdot E_{\text{glass}} \quad (1)$$

Assuming that the pre-stressed laminated glass beams are in equilibrium after all materials cooled back to room ambient temperature, the stress in the Fe-SMA strips $\sigma_{\text{Fe-SMA},120\text{min}}$ can be calculated with Equation (2), where $A_{\text{Fe-SMA}}$ and A_{glass} are the cross section areas of one Fe-SMA strip and of the laminated glass beam, respectively:

$$\sigma_{\text{Fe-SMA},120\text{min}} = \frac{\sigma_{\text{glass},120\text{min}} \cdot A_{\text{glass}}}{2 \cdot A_{\text{Fe-SMA}}} \quad (2)$$

It can be concluded that the applied activation procedure and the targeted heating temperature of 160 °C lead to a pre-stress of almost 7 MPa in the glass beams and of around 240 MPa in the Fe-SMA strips.

Table 4 Selected mean values (MV) and coefficients of variation (CV) from the temperature and strain measurements during activation of the Fe-SMA

Property	Mean value	CV [%]
Heating rate Fe-SMA [°C/s]	2.56	31.5%
$T_{\text{max,Fe-SMA}}$ [°C] (time [s])	162.0 (53.4)	2.1% (38.3%)
$T_{\text{max,glass}}$ [°C] (time [s])	37.4 (249.7)	8.3% (6.7%)
$\epsilon_{\text{max,glass}}$ [μm/m]	-437.1	12.3%
$\epsilon_{\text{glass},120\text{min}}$ [μm/m]	-95.6	11.2%
$\sigma_{\text{glass},120\text{min}}$ [MPa]	-6.7	10.8%
$\sigma_{\text{Fe-SMA},120\text{min}}$ [MPa]	239.4	11.2%

During activation two types of damages could be observed as shown in Figure 9. On the one hand, shear cracks in the glass occurred in some cases near the spacer gaps in the adhesive beneath which the copper clamps were fixed (see example in Figure 9c). This happened because the clamps were positioned on the interior side of this gaps, leaving only a small adhesive joint length before the gap for transferring the occurring shear forces. This could be very probably avoided in future either by positioning the clamps on the exterior side of the gaps or by filling the gaps with adhesive before activation. A second type of damage was observed locally at different points along the activation length in the form of debonding of the adhesive (see example in Figure 9b). This happened due to the heating. To avoid this in future, a slightly different order of the production steps could be adopted by: (i) first bonding the Fe-SMA strips to the glass edges only along the anchorage lengths, (ii) then activating the strips and (iii) finally bonding the Fe-SMA strips to the glass edges along the activation length.

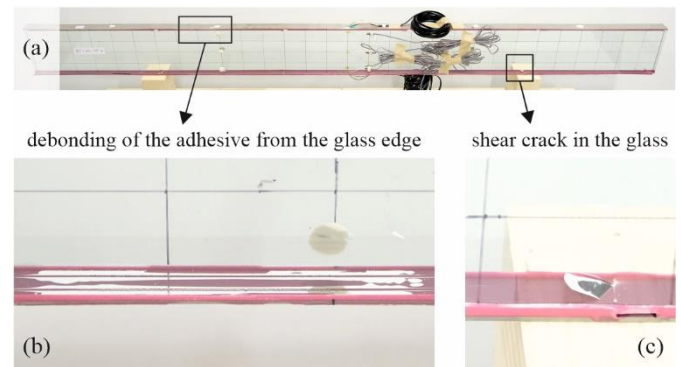


Figure 9 Overview of one of the pre-stressed laminated glass beams (a) with the location of debonding of the heated adhesive from the glass edge (b) and of a shear crack resulting in the glass (c) observed during activation of the Fe-SMA. Source: V.A. Silvestru/ETH Zurich

4.2 Four-point-bending results

The four-point-bending test results discussed in this contribution focus on the force vs. displacement behaviour as well as on the failure modes of the different types of investigated glass beams to emphasize the contribution of the adhesively bonded Fe-SMA strips to enabling a ductile failure of laminated glass beams. The force vs. displacement curves obtained from the tests on the nine glass beams are shown in Figure 10. In addition, Table 5 provides selected mean values and coefficients of variation from the tests to allow an even better comparison. For the laminated glass beams, it can be observed from Figure 10a that the bearable force drops significantly after the first

pronounced initial glass crack occurs. A low residual load-carrying capacity is provided on the tension side by the interlayer before it also breaks.

The curves in Figure 10b show that the reinforced laminated glass beams exhibit a significantly improved residual load-carrying behaviour after the first pronounced initial glass crack. There is still a drop in the bearable force, however, this drops is not as big as for the beams without reinforcement and the force is afterwards increasing again up to the capacity before initial crack or even a little higher. Furthermore, large deformations are occurring before ultimate failure. During these large deformations, additional cracks are resulting in the glass layers, which can be identified in the curves as drops of the force. The mean value of the force at initial glass crack is almost two times higher for the reinforced laminated glass beams compared to those without any reinforcement.

Figure 10c shows the force vs. displacement curves for the pre-stressed laminated glass beams. These beams exhibit in general a similar behaviour to the reinforced ones. Differences can be mainly observed when comparing the values in Table 5. The mean value of the force at initial glass crack is around 20% higher than in the case of the reinforced beams and a similar improvement can be observed also for the minimum bearable force after the initial glass crack. The mean values of the maximum force and displacement at the end of the tests are similar for the reinforced and the pre-stressed beams. However, one should know that for the reinforced beams, the ultimate failure occurred by rupture of the Fe-SMA strips along with some local adhesive debonding, while for the pre-stressed beams the tests were stopped due to large horizontal displacements at the sliding support before reaching an ultimate failure.

The values for the tensile stress in the glass at initial glass crack provided in Table 5 were determined based on the average of the strains measured with strain gauges SG03 and SG04. Therefore, the strains and implicitly the stresses directly at the glass edge, where the cracks initiate, were a little higher. The stress value for the laminated glass beams is lower than the characteristic bending strength of annealed glass (45 MPa), while for the reinforced and the pre-stressed beams the values are higher.

Figure 11 shows for each beam type representative images of the initial glass crack and the crack pattern at ultimate failure. These images confirm visually the already discussed results based on the force vs. displacement curves. Especially the image of the pre-stressed beam in Figure 10f, where ultimate failure was not reached, emphasizes the large possible deformations and implicitly the enabled ductile failure.

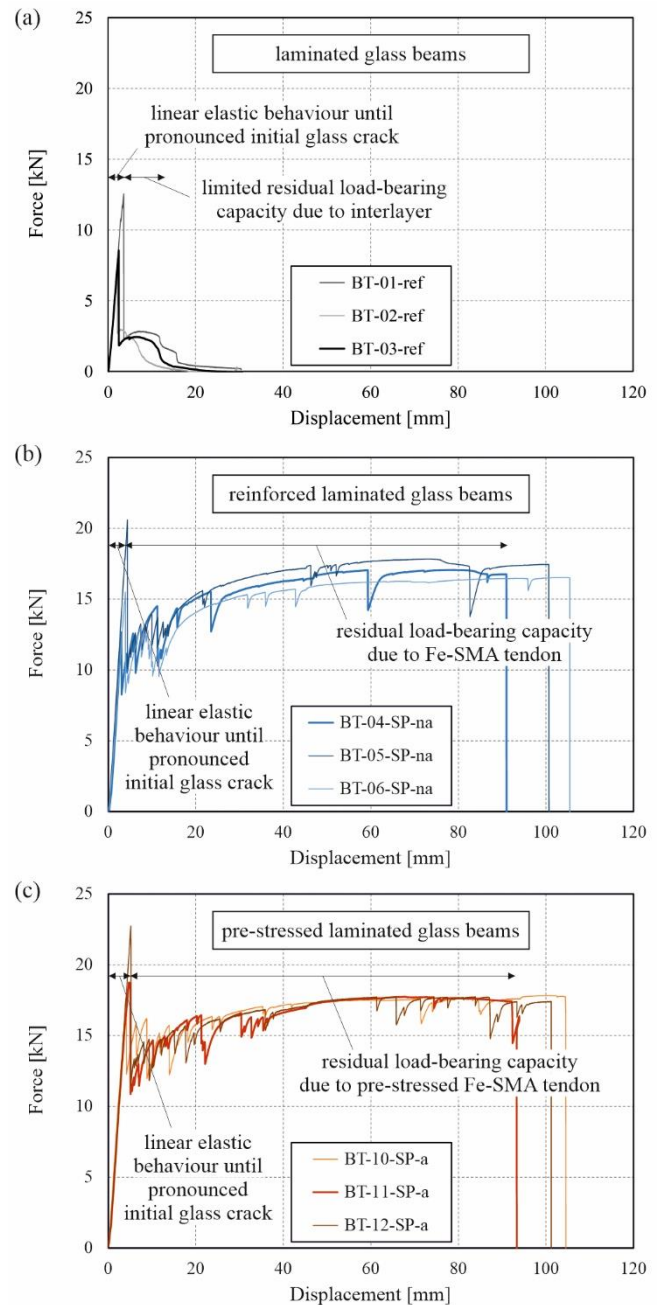


Figure 10 Load vs. displacement curves for the laminated glass beams (a), the reinforced laminated glass beams (b) and the pre-stressed laminated glass beams (c). Source: V.A. Silvestru/ETH Zurich

Table 5 Selected mean values (MV) and coefficients of variation (CV) from the four-point-bending tests

Property	Laminated glass beams		Reinforced glass beams		Pre-stressed glass beams	
	MV	CV [%]	MV	CV [%]	MV	CV [%]
Force at initial glass crack [kN]	8.3	27.5%	15.1*	17.3%	18.1	3.4%
Displacement at initial glass crack [mm]	2.3	24.0%	3.5*	11.5%	4.3	9.1%
Glass tensile stress at initial glass crack [MPa]	34.4	26.8%	52.9*	16.3%	63.0	3.7%
Minimum load after initial glass crack [kN]	-	-	8.9	11.6%	11.4	4.8%
Maximum load after initial glass crack [kN]	2.8	10.1%	17.2	3.8%	17.8	0.2%
Displacement at ultimate failure [mm]	14.0	26.8%	99.0	7.4%	99.7	5.8%

* BT-06-SP-na showed a fine crack in one of the glass layers at a lower load of around 6.7 kN. This was considered an outlier and was not included in the calculation of these values due to the different composition of the specimen with only one Fe-SMA strip adhesively bonded on the tension side.

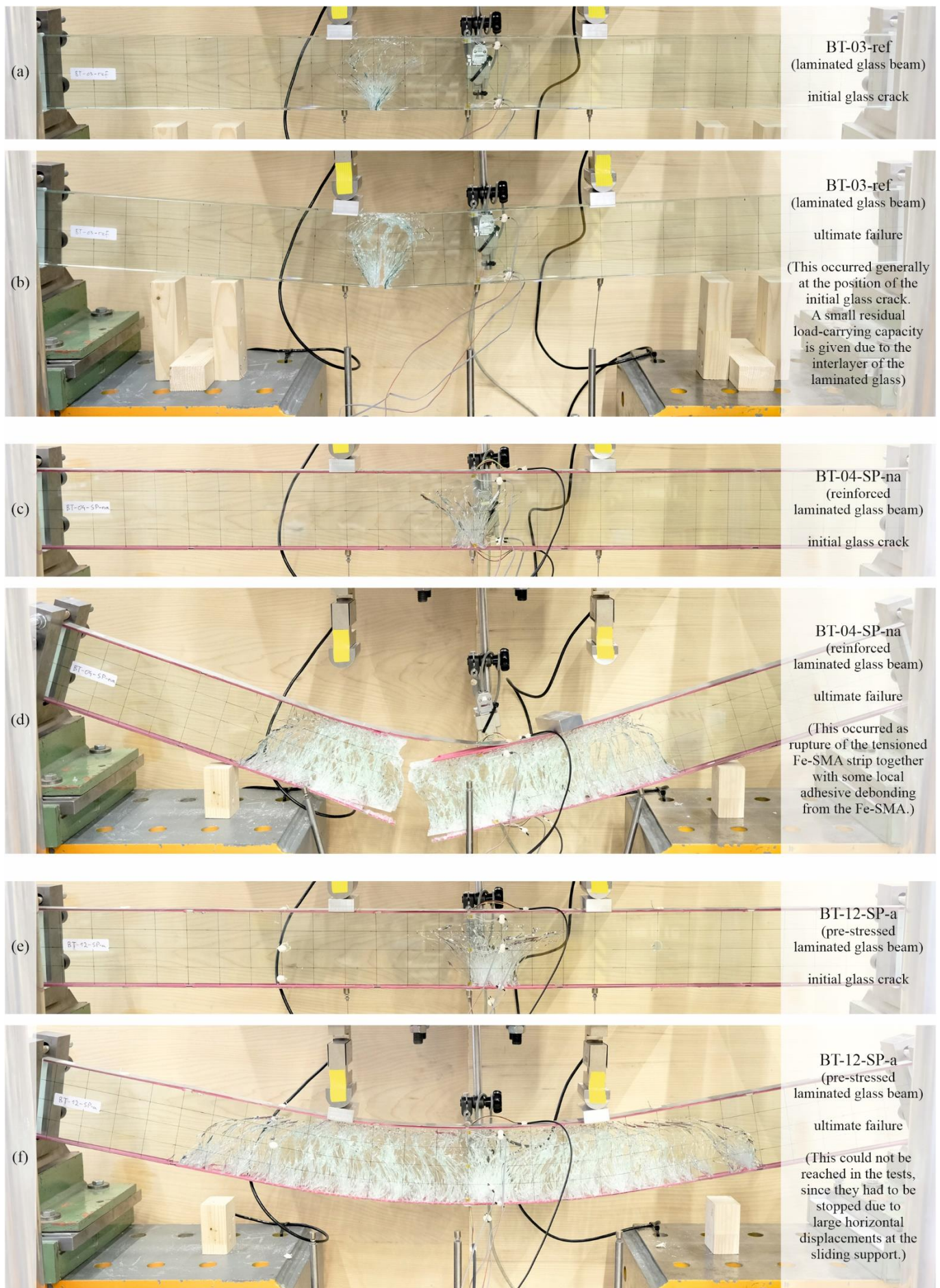


Figure 11 Representative failure developments showing the initial glass crack due to bending and the crack pattern at the end of the tests for a laminated glass beam (a-b), a reinforced laminated glass beam (c-d) and a pre-stressed laminated glass beam (e-f). Source: V.A. Silvestru/ETH Zurich

A comparison between Figure 11d and Figure 11f shows that the pre-stressing of the Fe-SMA strips leads to a spreading of the glass cracks over a larger part of the beam length. This indicates as well a better performance of the pre-stressed laminated glass beams.

5 Conclusions and outlook

In this contribution a novel concept is introduced for producing pre-stressed laminated glass beams by activating adhesively bonded pre-strained Fe-SMA strips. Based on analysing the pre-stressing procedure and performing four-point-bending tests on laminated glass beams, reinforced laminated glass beams and pre-stressed laminated glass beams, the benefits of the novel concept in improving the structural capacity as well as in increasing the residual load-carrying capacity and in enabling a ductile failure of laminated glass beams were shown. From the performed investigations and the obtained results, the following more specific conclusions can be drawn:

- The application of adhesively bonded reinforcement tendons made of pre-strained Fe-SMA strips along the edges of laminated glass beams allows a significant improvement of the initial glass crack force and especially of the residual load-carrying capacity in terms of bearable forces and reachable deformations before ultimate failure.
- An additional activation of the pre-strained Fe-SMA strips resulting in pre-stressing the laminated glass beams is possible by the method of electrical resistive heating. Compressive pre-stresses of around 7 MPa could be applied in the presented investigations.
- Pre-stressed laminated glass beams allow an additional increase of the initial glass crack force as well as of the minimum bearable force after this initial glass crack occurs, compared to reinforced laminated glass beams. The additional pre-stressing seemed not to improve significantly the maximum deformations and the maximum bearable force before ultimate failure, but it facilitates spreading the glass cracks over a larger part of the beam length.

Future investigations on pre-stressed laminated glass beams with adhesively bonded Fe-SMA strips should focus among others on essential open questions concerning (i) the long-term behaviour of such beams in terms of durability of the adhesive joints and preservation of the pre-stress level, (ii) the optimization of the anchoring and pre-stressing methods as well as (iii) the development of structural design approaches for such beams.

Acknowledgements

This research was conducted as part of the innovation cheque number 51447.1 INNO-ENG funded by Innosuisse – Swiss Innovation Agency and supported by re-fer AG, re-fer AG, Glas Trösch AG and Sika Schweiz AG are gratefully acknowledged for providing necessary materials for the test specimens. Furthermore, the authors would like to thank the laboratory staff of the Institute of Structural Engineering at ETH Zurich for their support in performing the experiments.

References

- [1] Martens, K.; Caspeele, R.; Belis, J. (2016) *Development of reinforced and posttensioned glass beams: Review of experimental research*. J. Struct. Eng. 142(5), 04015173.
- [2] Louter, C.; Nielsen, J.H.; Belis, J. (2013) *Exploratory experimental investigations on post-tensioned structural glass beams*. In: Cruz, P. (ed.) Structures and Architecture: Concepts, Applications and Challenges, 358-365, London: Taylor & Francis Group.
- [3] Jordao, S.; Pinho, M.; Neves, L.C.; Martins, J.P.; Santiago, A. (2014) *Behaviour of laminated glass beams reinforced with pre-stressed cables*. Steel Constr. 7(3), 204-207.
- [4] Engelmann, M.; Weller, B. (2016) *Post-tensioned glass beams for a 9 m spannglass bridge*. Struct. Eng. Int. 26(2), 103-113.
- [5] Bos, F.P.; Veer, F.A.; Hobbelman, G.J.; Louter, P.C. (2004) *Stainless steel reinforced and post-tensioned glass beams*. In: 12th Int. Conf. on Experimental Mechanics, 1-9, Bari.
- [6] Louter, C.; van Heusden, J.; Veer, F.; Vambersky, J.; de Boer, H.; Versteegen, J. (2006) *Post-tensioned glass beams*. In: Gdoutos, E.E. (ed.) Fracture of Nano and Engineering Materials and Structures, Dordrecht: Springer.
- [7] Schober, H.; Gerber, H.; Schneider, J. (2004) *Ein Glashaus für die Therme in Badenweiler*. Stahlbau 73(11), 886-992.
- [8] Cupac, J.; Louter, C.; Nussbaumer, A. (2021) *Flexural behaviour of post-tensioned glass beams: Experimental and analytical study of three beam typologies*. Compos. Struct. 255, 112971.
- [9] EN 572-1 (2016) *Glass in building – Basic soda-lime silicate glass products – Part 1: Definitions and general physical and mechanical properties*.
- [10] Kuraray (2014) *Physical properties of SentryGlas® and Butacite®*. Technical data sheet.
- [11] Ghafoori, E.; Hosseini, E.; Leinenbach, C.; Michels, J.; Motavalli, M. (2017) *Fatigue behavior of a Fe-Mn-Si shape memory alloy used for prestressed strengthening*. Mater. Des. 133, 349-362.
- [12] Izadi, M.R.; Ghafoori, E.; Shahverdi, M.; Motavalli, M.; Maalek, S. (2018) *Development of an iron-based shape memory alloy (Fe-SMA) strengthening system for steel plates*. Eng. Struct. 174, 433-446.
- [13] Silvestru, V.A.; Deng, Z.; Michel, J.; Li, L.; Ghafoori, E.; Taras, A. (2022) *Application of an iron-based shape memory alloy for post-tensioning glass elements*. Glass Struct. Eng., under review.
- [14] Wang, W.; Hosseini, A.; Ghafoori, E. (2021) *Experimental study on Fe-SMA-to-steel adhesively bonded interfaces using DIC*. Eng. Fract. Mech. 244, 107553.
- [15] SikaPower®-1277 (2019) *Toughened and high impact-resistant 2C structural adhesive*. Product data sheet, Sika Limited.
- [16] Izadi, M.; Hosseini, A.; Michels, J.; Motavalli, M.; Ghafoori, E. (2019) *Thermally activated iron-based shape memory alloy for strengthening metallic girders*. Thin-Walled Struct. 141, 389-401.
- [17] Shahverdi, M.; Michels, J.; Czaderski, C.; Motavalli, M. (2018) *Iron-based shape memory alloy strips for strengthening RC members: Material behavior and characterization*. Constr. Build. Mater. 173, 586-599.